Exploring the Role of Polymer Melt Viscosity in Melt Flow and Flammability Behavior

by

T.J. Ohlemiller, J. Shields, K. Butler,
B. Collins and M. Seck
Building and Fire Research Laboratory
National Institute of Standards and Technology
Gaithersburg, MD 20899 USA

Reprinted from the New Developments and Key Market Trends in Flame Retardancy. Fall Conference. Proceedings. Fire Retardant Chemicals Association. October 15-18, 2000, Ponte Vedra, FL, Fire Retardant Chemicals Assoc., Lancaster, PA, 1-28 pp, 2000.

NIST
National Institute of Standards and Technology
Technology Administration, U.S. Department of Commerce

Exploring the Role of Polymer Melt Viscosity In Melt Flow and Flammability Behavior[1]

Abstract

Thermoplastic polymers are widely used in roles where molding facilitates cost effective, high volume applications. Such polymers exhibit uniquely complex behavior in a fire because of their tendency to liquefy and flow. This behavior was explored in two stages. In the first, the melt behavior was examined in a non-flaming situation that subjected one face of a polymer slab to a radiant heat flux. The transient flow behavior was recorded for comparison to a model that uses the separately-measured melt viscosity as an input. In the second stage of the study, the burning behavior was examined in a facility that allows heat release rate measurements. These experiments explored the sensitivity of the evolved heat release rate to polymer type, polymer melt viscosity and physical aspects of the experimental set-up. The results demonstrate that the burning behavior of a thermoplastic object can vary strongly with the conditions under which it is burned if its melt viscosity permits appreciable flow.

Introduction.

In certain consumer product areas, such as electronic devices and automobiles, complex molded parts made from thermoplastic polymers are increasingly common. Low part costs for large production runs and the ability to integrate into one piece what formerly required several individual parts make this a trend that is likely to continue. Commodity polymers, such as polypropylene and polystyrene, which are used for these components are inherently flammable unless properly treated with flame retardants. However, there is a shift (initiated in Europe) occurring in the nature of acceptable flame retardants for ecological reasons. These two trends, the growth in thermoplastic components and the possible shift in the nature of flame retardants, provided an incentive to look at the flammability behavior of thermoplastics and to assess the extent to which this behavior may affect the appropriate choice of new means of flame retardancy. This paper reports on the first of these issues: an examination of the interaction of melt behavior with flammability of unretarded polymers. A study of the interaction of melt behavior with certain flame retardant approaches is planned for the future.

Experience with the burning of thermoplastic automotive components has demonstrated that it is a very complex process dependent on several factors [1]. The central complexity, long recognized, is that most thermoplastics change shape as they are subjected to the heat of the burning process. This is probably the chief reason why the

[1] T. J. Ohlemiller, J. Shields, K. Butler, B. Collins and M. Seck, Building and Fire Research Laboratory, National Institute of Standards and Technology Gaithersburg, MD 20899

literature contains few results in this area [2, 3, 4]. Time-dependent changes in fuel geometry make modeling of the burning process much more challenging.

Shape change is typically accompanied by the movement of hot, lowered viscosity material to some new location under the influence of gravity. This polymer "melt" may be burning, both as it moves and in its new location. Thus the growing fire on the part re-shapes it, moving heated material and this, in turn, alters the fire growth process. The net result can depend strongly on where the moving material comes to rest and on the thermal properties of the material on which it rests. Thus, for example, the polymer melt can form a burning pool near the original part location so that the flames from this pool interact with this burning part or, in the opposite extreme, the melt can fall a substantial distance and be quenched on a cold, heat absorbing surface, thus robbing the original fire of fuel. The heat release rate of such a thermoplastic part may thus vary strongly with the physical circumstances in which it is burned.

The above melt-related behavior is not seen when testing horizontal samples of material in the Cone Calorimeter. When one is assessing new flame retardant materials for thermoplastics, it is desirable to also look at them in configurations that evoke the full range of their likely real world behavior. Some modes of flame retardant action, such as the accumulation of a physical barrier layer on the burning surface, could be affected by melt flow.

As a first step along the above lines, NIST initiated a study of polymer melt behavior in a very simple configuration: a thick, vertically oriented slab. Before examining the actual burning process of such a vertical slab, we looked at an idealized version of it to see if this could be modeled. Since this is a learning process, we wanted to first demonstrate our ability to capture the essence of the flow problem before moving on to the burning problem with melt flow. Thus this slab of thermoplastic was subjected to spatially uniform radiative heating on one surface. This was done for two polymers, one of which behaved in a distinctly simpler manner than the other and is, therefore, the one we have modeled first, as described below. In the next step, also reported here, we performed a series of experiments on the burning process itself and its sensitivity to polymer and physical parameters.

Description of Experiments

Melt/Flow Experiments. Figure 1 is a sketch of the polymer heating apparatus. A panel heated by the burning of natural gas uniformly irradiated the front face of a polymer sample (5.7 cm wide by 25 cm high by 25 mm thick). The sample was insulated on its lateral edges and its back surface. Its weight was measured by a scale that supported the sample frame. This scale had a resolution of 1 g. Polymer melt material was captured by a pan atop a second scale after a free drop of about 30 cm. This scale had a resolution of 0.1 g. The temperature of both scales was monitored to assure that they did not heat significantly (insulation and shielding were used to prevent this).

Here and in the flaming experiments described below, thick samples were used to allow a focus on melt flow from the front surface rather than collapse of the whole sample body.

In separate experiments the radiant flux to the polymer samples was varied. The intent was to hold this flux constant during the exposure (which began with the removal of a water-cooled shutter). However, the panel showed an initial spike in its flux of 25 % or more above the test-average flux (apparently because of variation in the rate of radiative emission losses from the panel in the presence vs. absence of the shutter). The transient behavior of the flux was followed by a flux gage placed next to the sample; the initial spike decayed after about 2 min to 3 min. The time-average radiant flux (which is the value reported below) was varied from the lowest level at which the panel remained reasonably stable (ca. 8 kW/m^2) to flux levels somewhat less than those seen with flames burning on vertical walls (maximum here of 26 kW/m^2). The flux gage was calibrated against a standard and has an estimated uncertainty of ± 5 %. The exposure time was varied from 10 min at the highest fluxes to 45 min at the lowest.

At intervals during a test, a mechanically-supported thermocouple (0.05 cm dia. sheath; chromel/alumel) was inserted nearly tangentially into the outer portion of the surface melt layer to get a measure of this surface temperature. This was done at two heights on the vertical centerline of the sample, usually about 5 cm from the top and 5 cm from the bottom. There were small systematic differences between the measurements at the two heights which have not yet been analyzed; the average is reported here. The temperature readings from this thermocouple varied with its exact placement in depth (affecting the extent of lead wire wetting by the melt); the values reported are the maxima. There is insufficient information to assess the absolute accuracy of this result as a measure of melt surface temperature but it is believed to be reasonably representative. A single thermocouple (bare junction made from 0.013 cm dia. chromel/alumel wire) was placed at the back of the sample (near its center) at its interface with the 25 mm block of ceramic fiber insulation there. A single thermocouple (bare junction made from 0.013 cm dia. chromel/alumel wire) was also placed in the melt pool, just above the catch surface, near the point at which melt material flowed in.

Small flakes of thin Kapton[2] polyimide sheet material (0.013 mm thick; typically ca. 3 mm square) were placed onto the upper region of the melt surface at intervals to serve as a means for estimating the downward flow velocity of the outer surface of the melt. The behavior of these was recorded by a Hi-8 video camera. The data have not yet been analyzed in detail but the velocities are on the order of 1 cm/s.

Preliminary tests were performed with commercial grades of low density polyethylene, high density polyethylene and polypropylene. The two polyethylenes exhibited a skin-

---

[2] Certain trade names and company products are mentioned in the text in order to specify adequately the equipment used. In no case does such identification imply recommendation or endorsement by the National Institute of Standards and Technology, nor does it imply that the products are necessarily the best available for the purpose.

forming behavior during heat-up that rendered their subsequent melt flow erratic and very complex. Thus the work reported here has focused on polypropylene that shows only some yellowing during heat-up. The results below compare the behavior of a commercial polypropylene (weight mean molecular weight believed to be a few hundred thousand; here denoted as PP) and a low molecular weight polypropylene having a weight mean molecular weight of 23,000 (here denoted as 23KPP). (Note: this low molecular weight polypropylene is a research-grade material that no physical properties useful to commercial applications. It was chosen as an extreme example of a low viscosity polymer.)

The melt viscosity of the polymer as a function of temperature is a key determinant of its behavior in these experiments (and during burning). Polymer melts are non-Newtonian fluids; all of those used here exhibited shear thinning behavior. A controlled shear rate rheometer was used to measure viscosity as a function of temperature and shear rate in nitrogen.

Flammability Behavior Experiments. Figure 2 shows that a physical set-up similar to that in Fig. 1 was used for examining flammability behavior. The sample holder and sample scale are the same as above. Here, however, the sides (including top and bottom) of the sample holder had added insulation to minimize sample heating anywhere but on its face, even when pool fire flames came up around the sample holder. The tests were conducted under the hood of the original NIST Cone Calorimeter to allow measurements of the overall heat release rate as a function of time. The Cone heater was removed and no external radiative heating was used. Once again a single thermocouple (same as above) was placed at the back of the sample (near its center) at its interface with the 25 mm block of ceramic fiber insulation there. A single thermocouple (bare junction made from 0.013 cm dia. chromel/alumel wire) was also placed in the melt pool, a few centimeters in front of the plane of the sample face. Flaming across the width of the sample face was initiated with a 1.3 cm dia. tubular burner with small holes evenly spaced along it length. The burner was placed 1 mm to 2 mm from the outer edge of the sample frame, about 9 mm to 10 mm from the sample face. Methane was fed to the burner at a fixed rate sufficient to provide a flame height on the sample face of approximately 2 cm. to 3 cm. The methane flow was monitored with a rotameter and kept constant at the same level for most tests. The burner was left on throughout the test in all cases. (In tests with nylon samples, the burner was moved back to a distance of 2 cm and the methane flow was turned up to yield a flame height that reached about half way up the sample face.) The burner was placed either near the bottom of the sample face (ca. 1.3 cm up) or 2/3 of the way up the face to yield either predominant upward flame spread or downward spread. The catch pan was typically made from 1.3 cm thick calcium silicate board (Marinite) placed on top of small blocks that isolated it thermally on its bottom side. The peripheral edges were aluminum foil. The pan material was varied in a few tests described below in order to measure the impact of this parameter.

A feature of the system used throughout was a "drip lip" at the bottom of the sample holder. This was simply a piece of aluminum foil, slightly greater in width than the sample and ca. 2.5 cm long. It was shaped to help focus the melt flow toward the center

of the sample holder somewhat and it was also intended to help keep flames from trying to play heavily on the bottom or back of the sample holder. This lip may have played a role in one of the configuration comparisons described below.

The spacing between the bottom of the sample and the catch pan surface was varied between two values. In most tests a small spacing of between 2.4 and 4 cm allowed for strong interaction between the melt pool fire and the fire on the face of the sample. A larger spacing of 18 cm, which lessened this interaction, was used in two tests.

The heat release rate system was calibrated daily with methane at a known flow rate. A generic value was used for the heat release per unit mass of oxygen consumed; this limits the accuracy of measured heat release rates to a nominal value of ± 5 %. A more rigorous assessment of heat release rate measurement accuracy is a current subject of study.

All of the test configurations were run in replicate. Reproducibility was very good for the simplest-behaved polymer (PMMA); other materials showed variability of the order of ±10 % at any given time in heat release rate or other measured parameters.

All of the tests were videotaped to permit measurements of such variables as flame height or pool fire diameter. These tests included the same two types of polypropylene as used above; they also included commercial grades of polystyrene, PMMA and nylon 66. Only limited rheometry was done on these additional polymers.

Results and Discussion

Rheometry. All of the polymers used in this study were subjected to controlled shear rheometry; Fig. 3 shows the results. Tests were done at fixed shear rates of 5 s^{-1} or 10 s^{-1} while heating the sample at 2 °C/min. This level of shear rate was chosen as being comparable to that exhibited in the polymer melt flow experiments. No useful data could be obtained in this manner for either the nylon 66 or for PMMA, as their viscosity was excessive. The data for nylon 66 in Fig. 3 are from the polymer manufacturer and they were obtained in a forced flow-orifice rheometer at a shear rate of 100 s^{-1}. The PMMA manufacturer had no melt viscosity measurements on this polymer since it is too viscous for flow molding. Thus its position in the Figure is only roughly indicated. Note also that PMMA unzips as it degrades which means that it retains its high molecular weight and the viscosity would not be lowered by virtue of this type of change.

The 23KPP and PMMA clearly represent extremes of low and high melt viscosities, respectively. Viscosities of the other polymers fall much closer together but still vary by more than an order of magnitude.

The temperature window for rheometric measurements on all of these polymers was limited on the high side by rapid degradation that produces measurement-disrupting bubbles in the sample. On the low side it was limited by either the presence of a

crystalline phase in some cases or by excessively high viscosity. In retrospect the window on the low side could probably have been lowered by using a much lower shear rate but viscosity data above 1000 Pa-s are not particularly relevant to the present melt flow-related experiments. Flows that occur on the time-scale of the present experiments appear to involve viscosities below 100 Pa-s (and probably well below this level).

Thermogravimetry of these polymers at 2 °C/min in nitrogen indicated that all (except the nylon 66) were limited to the upper temperature ranges shown in Figure 3 by the onset of rapid degradation/gasification reactions. (PMMA would have been limited to less than about 250 °C had it been measurable.) Note that the experiments themselves may easily push the polymer surface layers beyond these temperature ranges and force further decreases in viscosity as a result of both increased temperature and decreased molecular weight effects. At present we have no way in which to assess melt viscosity in this domain.

The low molecular weight polypropylene was subjected to varied shear rate measurements (0.1 s^{-1} to 10 s^{-1}) at two fixed temperatures (170 °C and 200°C). At the lower temperature, the effect of shear rate was substantial with the viscosity increasing by a factor of three as the shear rate became very low. At the higher temperature, the effect of shear rate was negligible. This is in accord with the known tendency of polymer melts to behave in an increasingly Newtonian manner at sufficiently high temperatures. (Note that the viscosity of the nylon 66 would probably have been higher than that indicated in Fig. 3 had it been measured at a lower shear rate.) The temperature and shear rate dependencies of the 23KPP were fit to empirical functions that were used in the melt flow modeling described below.

Melt/Flow Behavior. Figure 4 shows the approximate steady-state mass loss rate from the two types of polypropylene as a function of the incident radiant heat flux. (The mass loss behavior was nearly steady for these tests but the values shown are those from late in each test where the loss rate was a maximum.) The commercial material was barely hot enough to begin to lose mass in a 45 min exposure at 8 kW/m^2; as the incident flux was increased, the mass loss rate became substantial. The 23KPP, on the other hand flowed freely, even at the lowest heat flux; this loss rate increased linearly with an increase in the flux, as a steady-state heat balance would suggest. Curves for both materials imply that the loss rate would be still greater if the heat flux were increased to the level (30 kW/m^2 to 40 kW/m^2) typically provided by flames on a vertical surface at this scale [5].

Figure 5 shows the average measured surface temperature values that go along with the mass loss rates in Fig. 4. Note that at equal heat fluxes the surface temperature of the 23KPP was as much as 200 °C less than that of the commercial PP. At the same time its mass loss rate was roughly twice as high. Reference to the melt viscosity data in Fig. 3 indicates the reason for these differences. The low melt viscosity of the 23KPP allowed its surface to reach only up to a temperature where rapid melt flow occurred. When this happens, the hot polymer melt running off the sample face carries away the bulk of the enthalpy deposited by the incident radiant heat. Figure 6 shows that for the 23KPP virtually all of the mass lost ended up in the melt pool. Thus essentially none of this low

molecular weight polypropylene degraded to gases at the surface temperatures achieved. A check on the melt viscosity of the material in the melt pool showed it to be essentially the same as the original material implying that little, if any, thermal degradation occurred. This qualifies the results with this polymer for comparison with the non-reactive melt flow model described below.

The data in Figs 4, 5 and 6 do not indicate that moving the heat flux up to levels typical of wall fires (ca. 30-40 kW/m^2; see Ref. 5) would change much of anything for the 23KPP polymer. The projected surface temperature at 35 kW/m^2 is about 250 °C. Our thermogravimetric data indicate that the polymer would be degrading at a low rate at this temperature (its TG mass loss rate peaked at 382 °C at 2 °C/min). Thus the data for this material imply that it would be difficult to make it burn in this vertical configuration because it tends to "melt" away at a temperature too low to provide sufficient gas phase fuel to the wall flames that would sustain the burning. The situation is more complex than this, as the flaming experiments below indicate.

Figure 6 also shows that slightly less than half of the commercial polypropylene ended up in the melt pool. The remainder was gasified. Rather surprisingly, the fraction gasified did not change appreciably as a function of heat flux even though Fig. 5 shows that the surface temperature was varying by about 150 °C over the flux range examined here (recall also the exposure time varies from 10 min to 45 min, inversely with the heat flux). Figure 6 implies that during burning about half of the commercial PP would feed a flame on the face of the sample and half would flow away to burn in a melt pool.

From a modeling standpoint, the 23KPP melt/flow behavior is distinctly simpler. The data here suggest that this experiment can be modeled without the inclusion of any degradation chemistry or gasification process. The commercial PP, on the other hand, degraded extensively in these tests. Viscosity measurements on material from its melt pool gave values much lower than on the starting material, implying a substantial decrease in molecular weight and, as was just noted, half of the weight lost went into gases.

Model of Melt/Flow During Radiative Heating. Polymer melt flow behavior like that measured above is complex; even the simple two-dimensional configuration studied here poses a challenge to the modeler. The most basic description must include equations of mass, momentum, and energy, with an imposed heat flux to raise the temperature of the polymer and gravity to drive the flow. The geometry of the problem changes significantly with time. The surface of the melt is a free surface that may undergo considerable deformation, including dripping, and the internal interface between the solid and melted polymer changes its location as the material heats and flows. The regions of flow are determined by the polymer melt viscosity, which, in general, depends strongly on temperature, molecular weight, and shear rate. If the temperature increases to a value at which gasification begins to take place, the model must add chemical reactions to the equations of heat and mass transport. The material properties of the vertical holder also affect the heat transport and therefore the flow.

The melting and dripping behavior of a polymer in this experimental study can be modeled using the "filling" capability of the commercial finite-element program FIDAP [6]. This software provides the means to model flow processes involving arbitrary changes in shape, including breakup and merging of fluid volumes. Free surfaces are described using a volume of fluid (VOF) method, in which a marker concentration field variable (denoted as "FILL") is set to unity within the fluid of interest and to zero outside. The free surface itself is located by steep gradients in the marker variable. The solution proceeds by alternate applications of Galerkin finite energy techniques to solve for mass, momentum, and energy and the VOF method to determine the new locations of free surfaces. The local mobility of the fluid depends on its viscosity, whose empirically-determined value as a function of temperature and shear rate is included in the problem by means of a user-defined subroutine. The polymer behaves as a solid where the viscosity is very high, and the melt front within the polymer can be located by the deepest nonzero velocities.

At present, we are focused on applying this approach to the non-reactive case which here means the 23KPP experiments summarized above.

Figure 7 shows the two-dimensional geometry and finite element mesh used for simulating the behavior of the 23KPP. The fineness of the spatial grid is dictated by the thinness of the flow layer that develops and by the need to resolve the details of any induced shape changes. The polymer sample is initially a solid filling the rectangular region above the lip that holds the sample in place. The model space also contains an initially empty region through which the polymer may flow before dripping into the catch basin. To determine the flow rate, mass loss rate, and surface temperature of the melting polymer it is not necessary to include the catch pan in the model. No-slip boundary conditions are applied to the back surface of the polymer on the left and to the solid lip below the sample. A radiative heat flux is applied to the melt surface and the back wall is insulated. Radiative and convective losses at the surface are calculated by a user-defined subroutine. The gravity force is directed downward. The fine spatial grid and the related small time steps necessitated by the flow make the solution process slow; it requires several hours of time on a work station computer.

The calculated evolution of the profile of the melting and dripping polymer with time is shown in Figures 8 and 9 for incident radiant heat fluxes of 12.5 and 20 kW/m^2 respectively. The position of the front face of the polymer is determined numerically by the location of the FILL=0.2 contour line. The flow is less smooth for the higher imposed flux; small traveling waves of melted material are visible in Fig. 9 at 100 and 200 seconds. In Fig.10, the mass of polymer remaining in the region, calculated by integrating the FILL variable over space, is plotted as a function of time. This should give a reasonable estimate of the sample mass with time to compare with experiment. The calculated quasi-steady state mass loss rates for fluxes of 12.5 and 20 kW/m^2 were 0.37 and 0.49 g/s, respectively. The mass loss rate agrees with experimental results in Fig. 4 for 23KPP heated at 20 kW/m^2, but is about 20% higher than the experimental value for 12.5 kW/m^2. Considering the uncertainties in the thermal properties of the

polymer and other aspects of the experiment, this level of agreement is quite encouraging. More detailed comparisons are planned.

The free surface capabilities of the FIDAP software enable the model to consider the behavior of the melt after it has fallen away from the sample holder. As will be seen below, this is an important aspect of an actual fire situation. Figure 11 shows the dripping of a melting PP sample into a catch basin over the first 100 seconds of heating at 20 kW/m^2. No-slip and simplified heat flux boundary conditions are applied to the catch basin surfaces. Since melted material must traverse no more than a single element during one time step in order to maintain numerical stability, the computation time necessary to solve this problem over a specified time period may increase considerably during each drip.

In order to simulate the melting and dripping behavior of the commercial polypropylene studied in the above experiments, the chemical reaction responsible for polymer gasification is currently being added to the model through the addition of species equations. Further species equations and user-defined subroutines will enable the investigation of burning polymers, non-Newtonian effects, and conditions under which the molten polymer that has dripped from the sample continues to burn and contribute to the overall heat release rate.

Flammability Behavior. The goal of these flammability studies was to assess the sensitivity of thermoplastic polymer burning to both polymer and physical parameters. As explained in the Introduction, we expect the melt behavior of the polymer to influence its burning behavior in a vertical orientation. The chemical nature of the polymer will also affect its relative tendency to yield flaming melt/drip material. Furthermore, the observed behavior depends, as well, on where the melt material goes and the ease with which it can burn and feed some of its flame heat back to the original polymer sample. Finally, there will be some impact of the location of the igniter on the face of the sample since this determines whether fire growth on the sample must be by upward or downward flame spread. Both of these spread modes are affected by the melt viscosity of the polymer. The apparatus sketched in Fig.2 allows us to explore all of these variables. Given the additional complexities that the burning process produces, we have not yet begun to model it.

Figure 12 shows an example of the time-dependent data collected from a typical fire. This is for a regular (not low MW) polypropylene, placed just above a calcium silicate board as the catch pan; the methane igniter was placed just above the lower edge of the sample face. Note the time scale on the plots. These are rather slowly-developing fires. This is not an inherent property; it is a consequence of the choice of a thick (2.54 cm) sample and a rather small igniter. Below it will be seen that other factors affect the speed of development, also.

Ignition of the sample face region directly impacted by the burner took less than one minute. The attached flames then began to slowly creep up the sample face with an indistinct attachment front that was difficult to follow precisely. By 200 s, molten

polymer began to drip onto the catch pan where it tended to "freeze" and pile up somewhat. As more drips arrived they were evidently somewhat hotter and the catch surface somewhat warmed; molten material began to persist and form a slowly spreading pool. By 600 s the molten polymer droplets were flaming as they reached the melt pool; at this time the flames on the sample face were attached to about half of the sample height. Flames began to persist (rather than flash) on the pool only after about 1000 s. Flames on the sample face were still attached only about half way up. The pool behavior throughout this test was complex; it "froze" on its outer edges, forming a dam which was then breeched erratically in time and place by lobes of melt, likely driven by surface tension gradients and gravity. As the pool fire grew (see width in the top graph), a self-accelerating process was initiated in which the pool flames boosted the fire growth on the sample face and the rate of melt arrival on the catch pan. The pool fire thus boosted its own growth rate and the overall heat release rate from the pool plus sample face fire grew in an accelerating manner. The fact that all elements of the system were increasing in temperature added to this tendency (e.g., note the back surface temperature of the sample). The test was terminated when the fire plume began to appreciably exceed the flow capacity of the hood above it.

Figure 13 shows a plot of the heat release rate versus time for all five polymers, using the same configuration as above. There is a wide variety of behavior here influenced by the melt characteristics and the thermo-chemical properties of these polymers. The thermo-chemistry differences include variations in heats of gasification, heats of combustion and in soot production which influences the heat feedback flux from the flames to the burning surface. Data from Ref. 7 do not cover the full set of polymers here but they do indicate that, in steady burning of a large, horizontal sample, one would expect the greatest heat release rate from polystyrene, then polypropylene, then PMMA. Polystyrene is rather uniquely high in its soot production; this appears to account for its high flame feedback flux that boosts its burning rate [7]. The experiments here are all transient and the behavior of the vertical samples is influenced by gravity-induced flow; nevertheless, Fig.13 shows that these same tendencies in heat release rate come through here.

PMMA is the only material that did not yield a melt pool at all. As implied by Fig. 3, its melt viscosity was so high as to overcome the force of gravity. The initial higher slope part of the curve is due to increasing involvement of the sample face via upward flame spread. The subsequent steady increase in heat release rate is due to the increasing pre-heating of the bulk of the sample; its back surface temperature reached about 230 °C by the end of the test.

Nylon 66 was reluctant to burn at all in these experiments, which included no external radiant flux. Note that the burner had to be pulled back somewhat from the surface to avoid clogging by the melt and the methane flow rate to the igniter was turned up to yield a flame that was somewhat more than half of the sample height. Thus the immediate heat release rate level of 1.2 kW to 1.3 kW comes strictly from the igniter (on throughout the experiment, as in all other tests). The melt tended to solidify as soon as it left the drip lip at the bottom of the sample holder (nylon has a crystalline phase with a melting point of ca. 265 °C). The drips eventually accumulated into a localized layer roughly 2 cm deep

layer there that burned weakly on its top. At 1200 s the burner was rotated about its axis to point its flames more toward the drip lip and its flowing layer of melt. The pool fire eventually grew to roughly 7-8 cm diameter; there was never any indication of flame attachment to the sample face or of upward flame spread on that face. Evidently the melt flow was effective in keeping the sample face temperature down below its ignition point.

A similar phenomenon protected the face of the 23KPP. Recall that the polymer melt flow experiments described above led us to expect this behavior for this polymer; it was noted that it flowed readily at a temperature too low to even degrade it significantly. This polymer does not re-solidify so readily as the nylon, however. Differential scanning calorimetry showed that its crystalline phase melts at ca. 130 °C. Thus the melt, flowing rapidly onto the catch pan, tended to stay molten and spread out. For the first 900 s this is all that happened. By this point the igniter flame melted through the full depth of the sample in front of it. This meant that melt from higher on the sample flowed down over the insulated aluminum foil backing past the igniter flame. With no polymer to act as a heat sink behind it, it reached higher temperatures and ignited in this region[3]. The flaming melt was carried onto the horizontal pool and immediately began to ignite it as well. This process was self-accelerating as the growing melt pool flames assisted the flames on the foil in melting more of the sample, further up its height. The pool fire grew rapidly and the entire sample was melted into it, yielding a large fire. As predicted above, flames never spread upward on the sample face or even ignited the face itself. This did not preclude a large fire, however.

The melt flow experiments above indicated that the normal, commercial polypropylene would degrade and gasify extensively at fire level heat fluxes, even as about half of the material melted and flowed downward. The behavior of this polymer was described above in the context of Fig. 12. Essentially, this polymer allowed slow, limited upward flame spread on its surface (to about half the sample height) until the pool fire began to contribute its supplemental heat feedback to the sample face. The fire then grew large at a self-accelerating pace. Thus the melt flow temporarily halted fire spread on the sample until it was overwhelmed by the pool fire that the melt fed.

Polystyrene, as indicated above, is expected to be the most flammable polymer here, as measured by its steady-state burning rate in a horizontal configuration. Its behavior in these vertical burn tests was complex but, overall, it lived up to the expectation. It is a strongly sooting polymer and it quickly coated the sample face with a layer of soot that may have had some insulative (and thus protective) effect. In any event, though it ignited locally within 30 s, no appreciable upward flame spread followed and this was not a result of downward melt flow. There was some indication of an oxidative skin forming on the hottest region of the face which retarded melt flow. Polymer melt began to drip to the catch pan only after about 300 s. The drips were flaming. A unique feature of the growing melt pool fire that developed immediately was the fact that its entire surface was burning from the beginning. (This tended to happen to the two polypropylenes only very

[3] One can anticipate that the 900 s delay seen here before the sample melted through and ignited would vary directly with sample thickness. A different sample holder configuration might also affect the ability of the flowing melt to ignite after sample melt-through.

near the end of a test.) The early development of the self-accelerating fire was probably slowed by the physical presence of the igniter. The molten material on the sample face sagged out against the burner, which thereby inhibited its flow onto the pool. This also tended to block the pool fire flame contact with the sample face. The fire began to accelerate strongly only after this melt material was physically removed. Another unique feature of the burning behavior of this polymer was the compactness of the pool fire. Even at the end when the heat release rate was at a maximum, the pool fire area was roughly comparable to that of the sample face. For the polypropylenes, by contrast, the pool fire tended to grow substantially larger than the area of the sample face as the heat release rate climbed. Evidently, the somewhat higher melt viscosity of the polystyrene (Fig. 3) slowed the mass loss rate by melt flow and facilitated more material burning on the sample face.

The importance of the melt pool fire to the overall fire development process was explored in a limited manner. For the commercial polypropylene, the sample was moved up higher above the catch pan; a distance of 18 cm (vs. the previous separation of 2.4 to 4 cm) was the largest that the apparatus would permit. The idea here was to limit the interaction between the melt pool fire and the sample face and thereby to limit the self-acceleration aspect of these types of fires. Figure 14 shows the measured results for the closely spaced and widely spaced cases. In the latter case, it was apparent after about 500 s that the drip edge at the base of the sample served as a surface on which some of the flowing melt could burn; in this sense, it served as a small "pool" fire (its effective area was roughly 15 cm^2) which remained closely coupled to the sample face and aided in its fire development. The real melt pool, 18 cm below, did not begin to burn steadily until about 1700 s and at this point its flames were only roughly about 6 cm tall. Note that this is the time at which the two curves in Fig. 14 start to diverge. By the end of the test in which the separation was 18 cm, the pool fire flames were frequently spanning the gap and reaching the bottom of the sample face. The separation was thus clearly not as great as desired and some weak self-acceleration probably persisted in the 18 cm separation case. The lesser heat release rate for this case does tend to confirm that heat feedback from the pool fire is an acceleratory mechanism for thermoplastic melt/drip fires.

Another potential way in which to affect the interaction between the pool fire and the sample face is by changing the nature of the catch pool surface. In principal, the melt material which falls onto the catch surface is subject to heat losses to that surface which should influence how readily it can begin to burn. The effect may be tempered by the self-insulating nature of the polymer material itself. That is, if the initial material solidifies in place due to heat losses to the surface on which it sits, the melt material that then falls on this solidified layer is insulated by it from that cold surface.

Figure 15 shows the results, with the commercial polypropylene, of varying the melt pool catch surface; the sample is once again placed down close to this pool surface. The middle heat release rate curve is the same as was seen before; it pertains to the calcium silicate catch pan surface used in all of the previous tests. The lower curve is for a catch surface made from a 1.27 cm thick aluminum plate, a very substantial heat sink, given

aluminum's high thermal conductivity. The upper curve is for a catch surface of the lowest thermal mass that could be devised; a sheet of 0.0025 cm thick stainless steel foil on top of a 0.6 cm thick layer of ceramic felt insulation. Clearly the effect of the catch surface on the rate of development of a this type of self-accelerating fire can be considerable. However, the range of materials used here could not eliminate this process; even the aluminum plate eventually began to heat up to the point where it could accommodate a growing melt pool fire. The results with polystyrene on aluminum vs. calcium silicate catch surfaces were approximately similar: the aluminum plate slowed the fire development by about 1000 s compared to that seen with a calcium silicate surface.

Finally, the effect of moving the igniter higher up on the sample face was explored with both the commercial polypropylene and with polystyrene. The igniter was placed about 2/3 of the way up the sample face, leaving 16-17 cm of unheated polymer surface between it and the bottom of the sample. The calcium silicate catch surface was another 4 cm below this. Both of these polymers showed a ready tendency for downward flame spread on this unheated surface as flaming melt flowed downward. The dynamics of this were complex since the melt solidified after some travel distance. The net effect for both polymers was to slow down the self-accelerating stage of the interactive pool-plus-sample-face fire by 200-300 s. This delay is presumably proportional to the downward travel distance for polymers that yield flaming melt flows on their face.

Summary and Conclusions

In the first part of this study, it was demonstrated that the melt flow characteristics of a thermoplastic polymer in a vertical configuration can have a strong effect on its reaction to an imposed heat flux. If the polymer melt is sufficiently fluid, the melt may carry away essentially all of the imposed heat at such a low temperature that the polymer does not degrade. If the melt is less fluid, a large fraction of the polymer mass may still flow downward off of the sample face. This has the potentially useful tendency to slow the upward flame spread on the polymer but it also puts a large amount of mass into a melt pool whose location may vary.

Modeling the simplest case of non-reactive melt flow, using an empirical description of the non-Newtonian melt viscosity, appears manageable but the problem is surprisingly computationally intensive due to the length and time scales involved. It remains to be seen whether the more complex cases of degradative melt flow and of burning can be managed in a reasonably efficient manner.

The burning melt/flow problem introduces new complexities. The behavior seen varies with the polymer type, the melt viscosity of polymer, the position of the melt pool relative to the sample and the thermal heat-sinking properties of the surface on which the melt pool lies. Clearly, the fire behavior of a vertical thermoplastic is substantially more complex than the typical characterization of materials as is done, with horizontal samples,

in the Cone Calorimeter, for example. The Cone offers external radiation as an additional realistic parameter; that was missing from the tests performed here.

Real products made from thermoplastics can be expected to exhibit the types of complex fire behavior seen here. This then is the context in which the flame retardant systems in these materials must function. If the flame retardant mechanism is affected by melt flow, it would be good to know this and to learn how to design around it, given an understanding of the impact of the parameters of the problem.

Acknowledgements

The authors would like to gratefully acknowledge the support of the Fire Retardant Chemicals Association for Brian Collins and Momar Seck. The authors are also grateful to Alex Morgan of NIST for the thermogravimetric measurements on the polymer samples.

References

1) Ohlemiller, T. and Shields, J., "Burning Behavior of Selected Automotive Parts from a Minivan," National Institute of Standards and Technology NISTIR 6143, August, 1998

2) Zhang, J., Shields, T. and Silcock, G., *Fire and Materials* **21**, pp 1-6 (1997)

3) Zhang, J., Shields, T. and Silcock, G., *J. Fire Sciences* **14**, pp 67- 84 (1996)

4) Kashiwagi, T., Omori, A. and Brown, J., "Effects of Material Characteristics on Flame Spreading," Fire Safety Science - Proceedings of the Second International Symposium, International Association of Fire Safety Sciences, Hemisphere Publishing, New York (1989) p. 107

5) Quintiere, J., *J. Res. Nat'l Bur. Stds.*, **93**, pp. 61-70 (1988)

6) *FIDAP 8 Theoretical Manual*, Fluent, Inc., Lebanon, NH, 1998.

7) Tewarson, A., *SFPE Handbook*, (2nd ed.) published jointly by NFPA and SFPE (1995), Section 3, Chap. 4

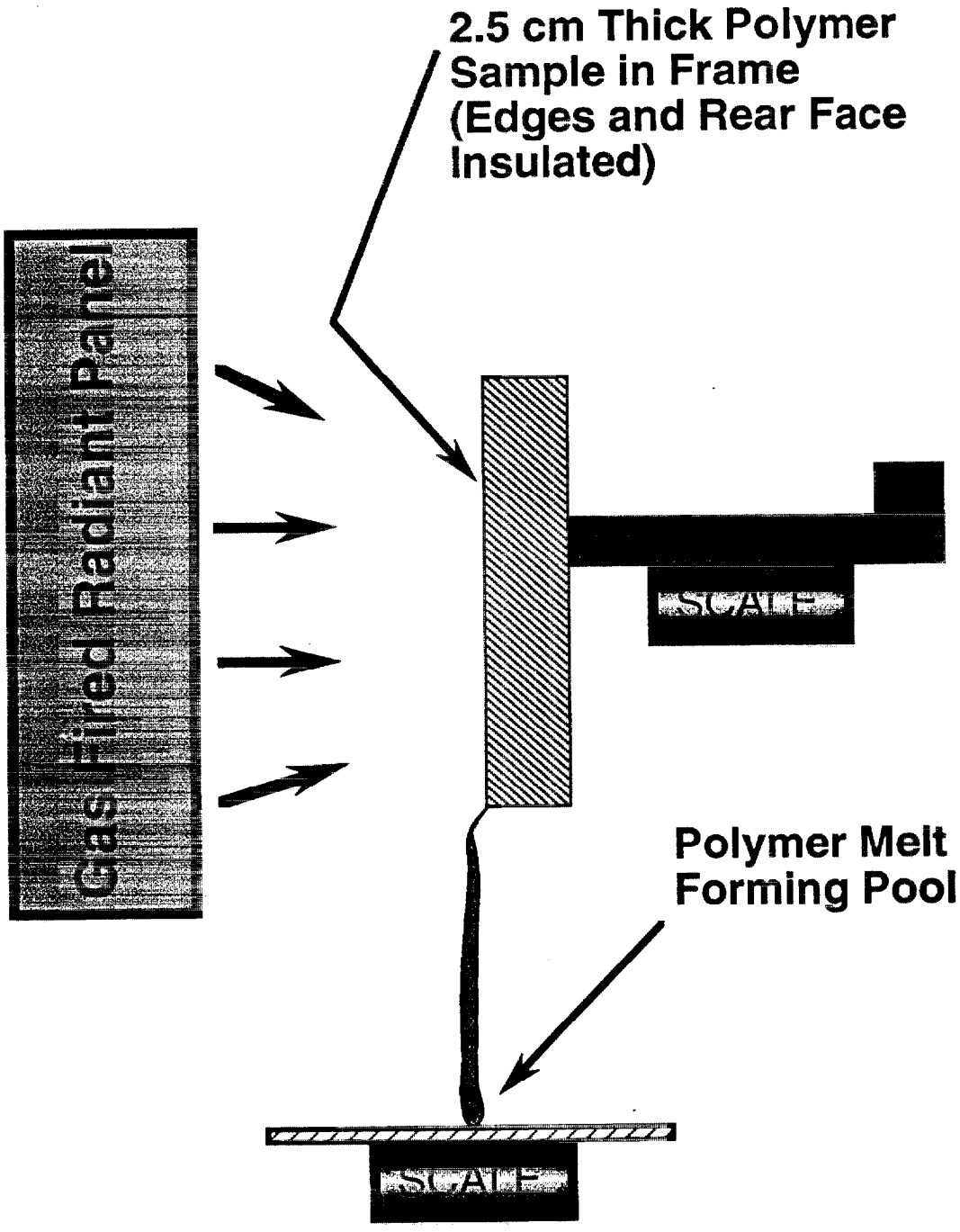

Figure 1. Polymer Melt Apparatus

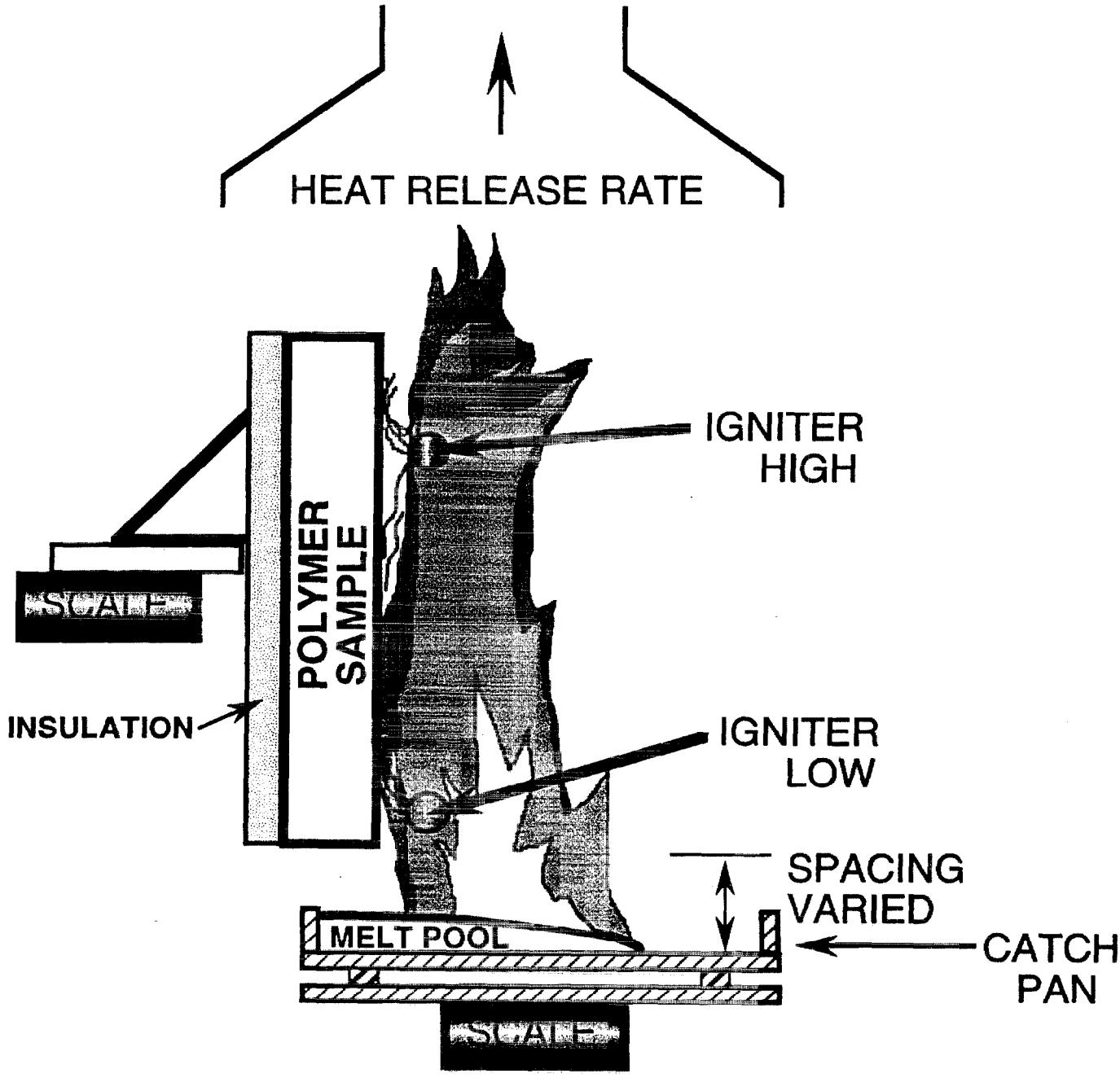

Figure 2. Experimental set-up for polymer melt-drip fires.

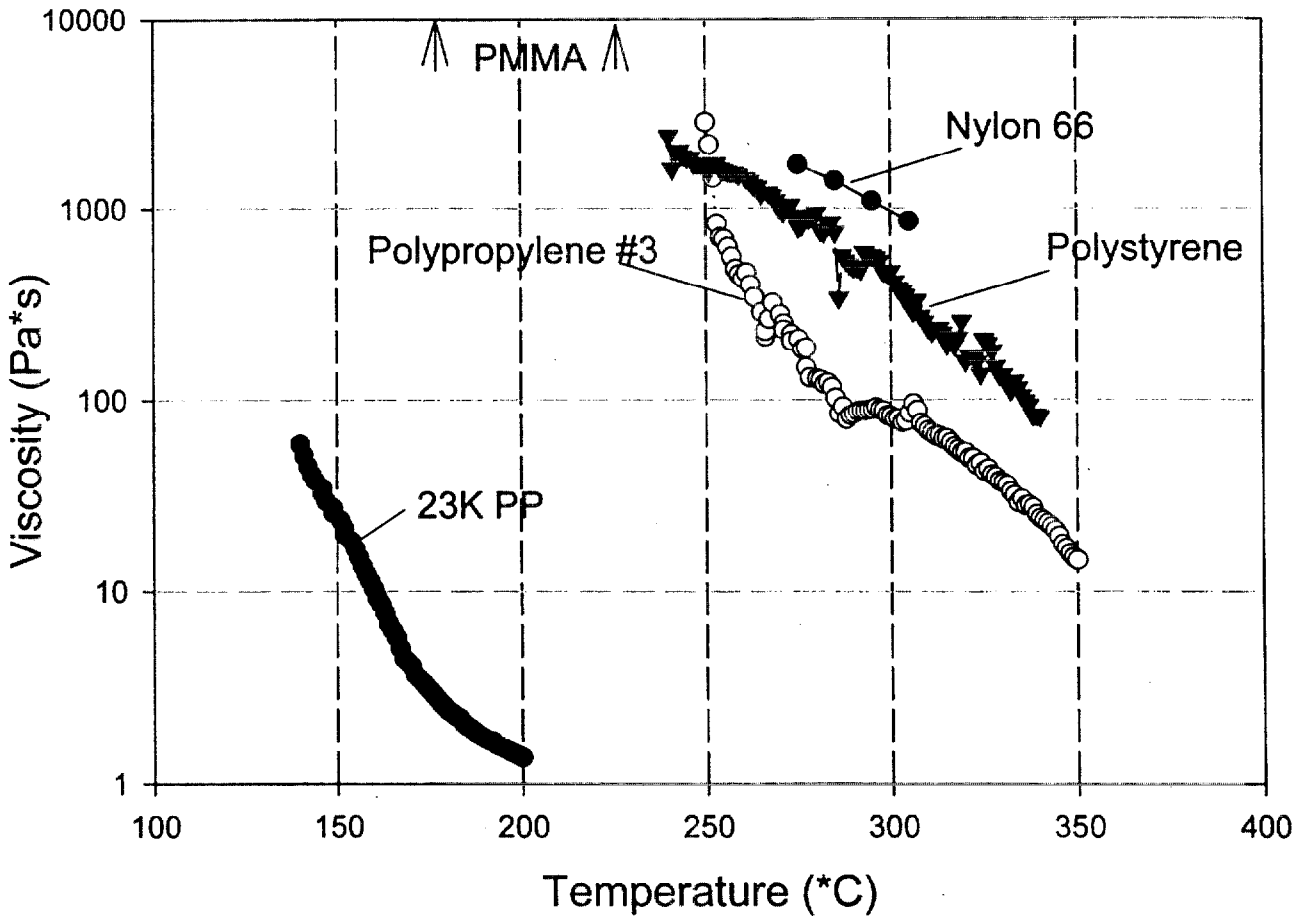

Figure 3. Melt Viscosity vs Temperature for polymers in this study

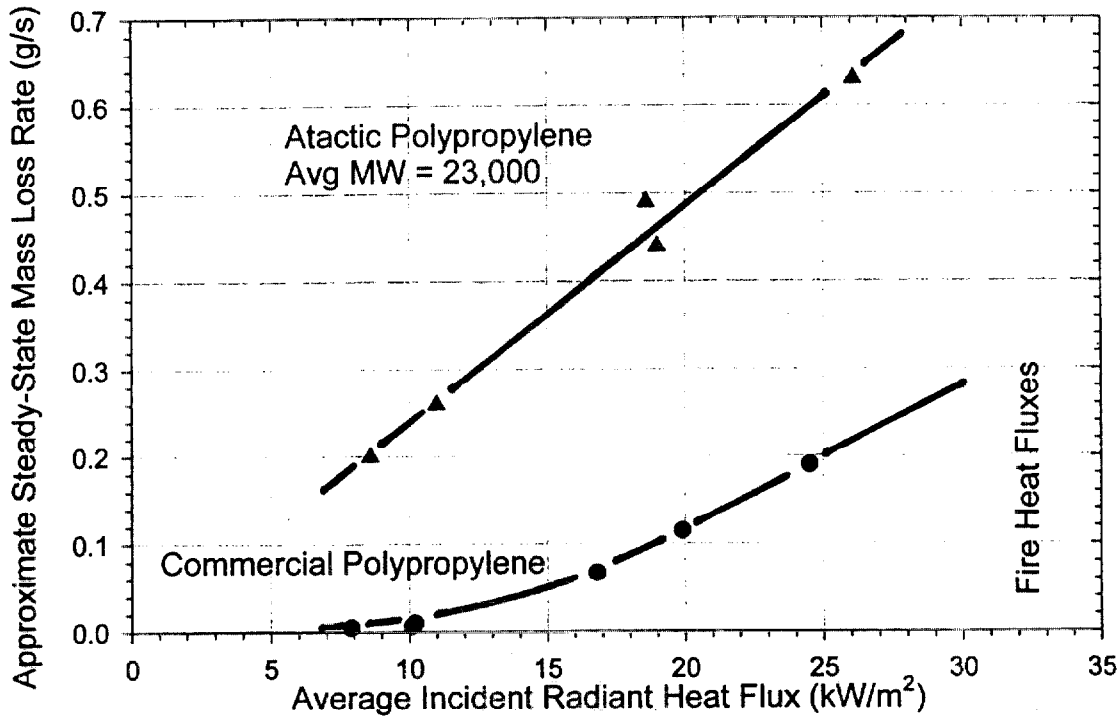

Figure 4. Steady-state mass loss rate from two types of polypropylene as a function of incident radiant heat flux.

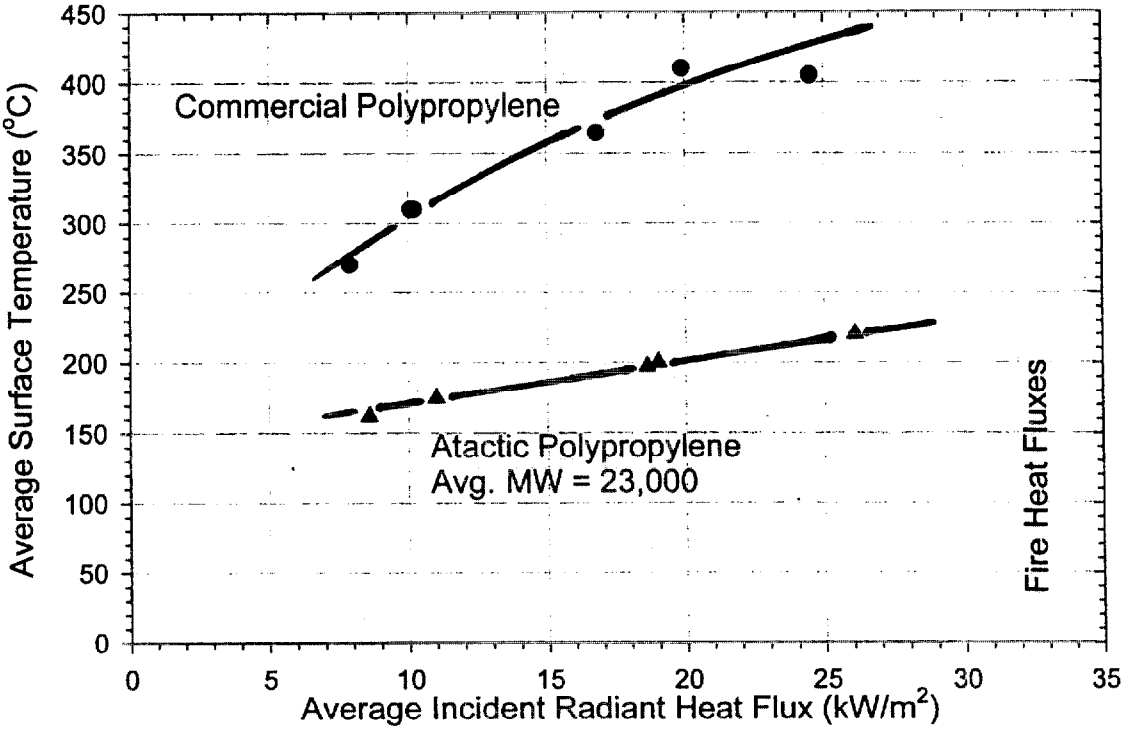

Figure 5. Average surface temperature for two types of polypropylene as a function of incident radiant heat flux.

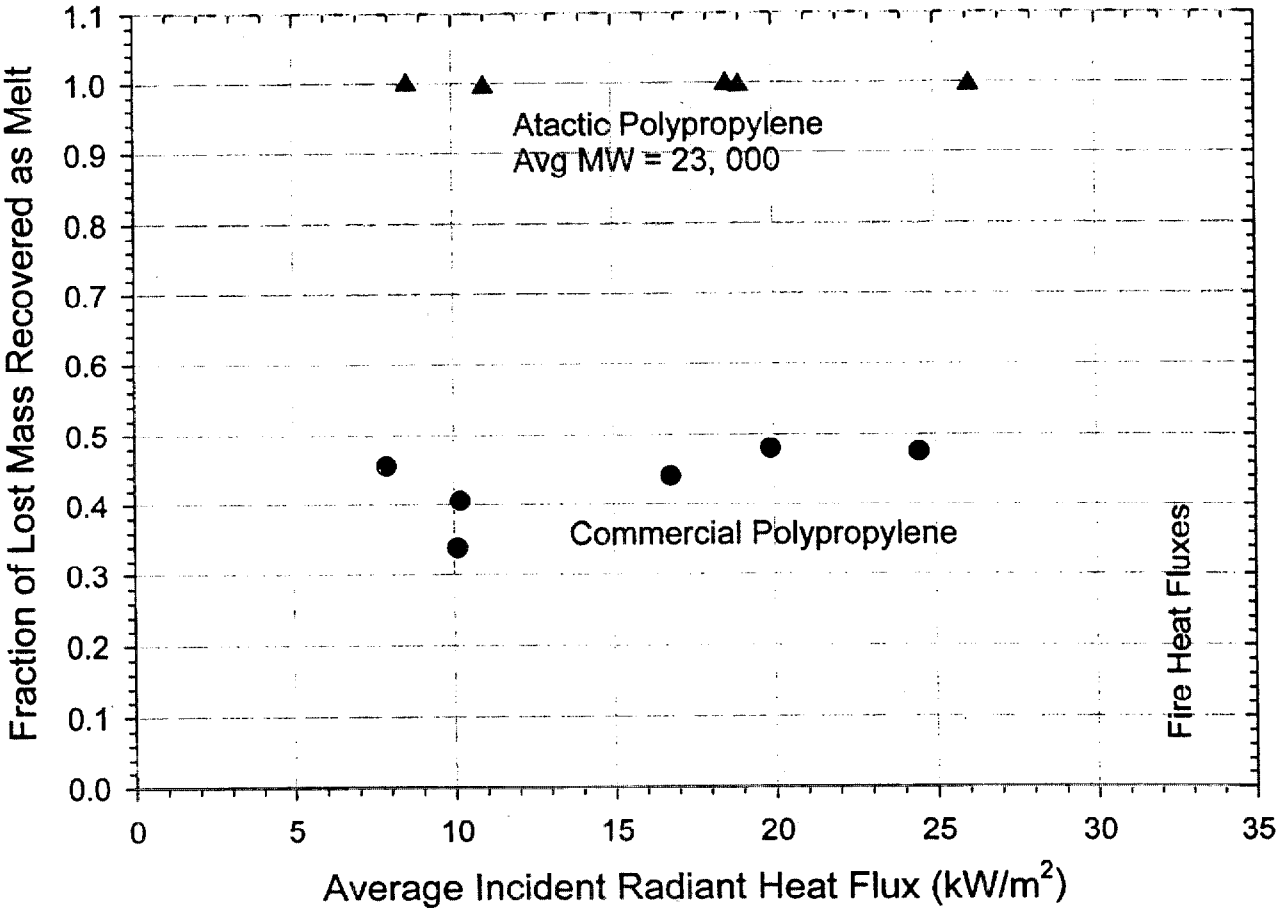

Figure 6. Fraction of sample mass loss that is recovered in the melt pool, as a function of incident radiant flux on sample face. Results for two types of polypropylene.

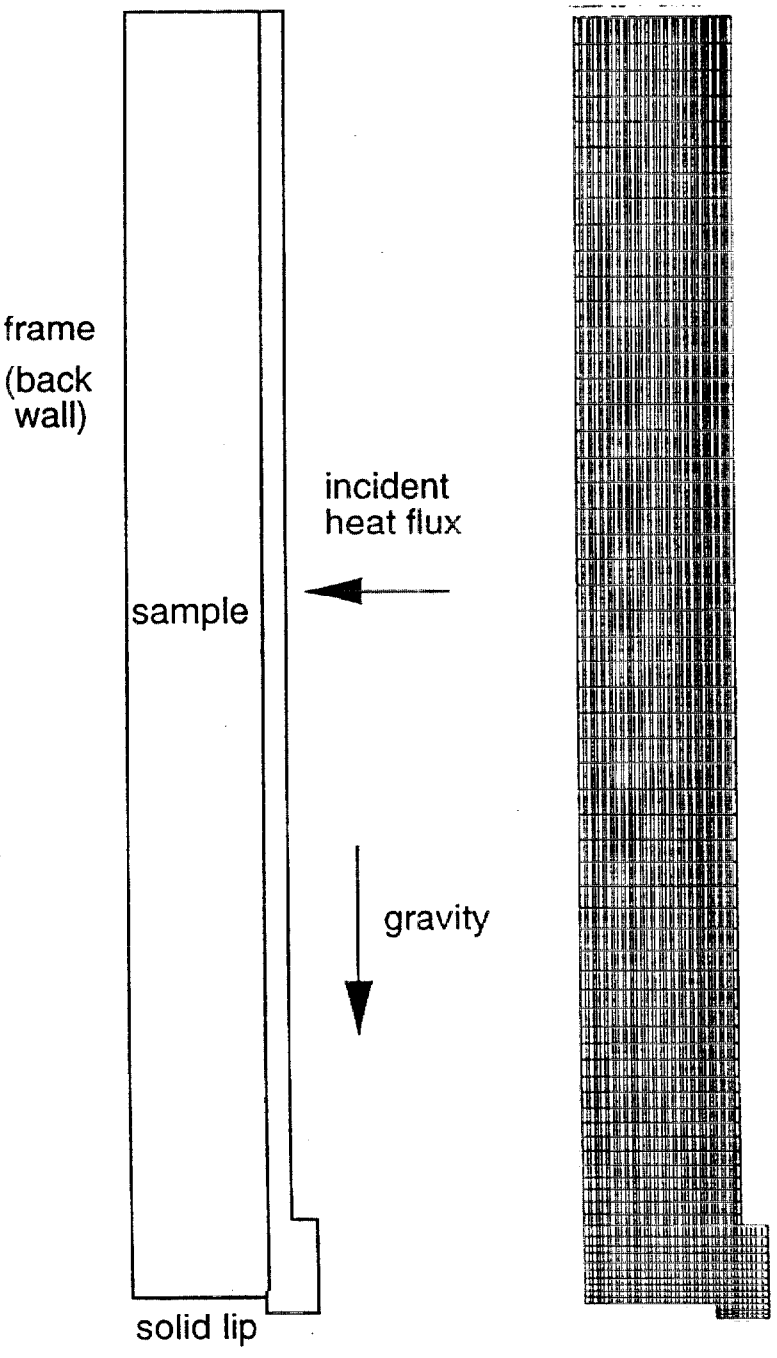

Figure 7. Geometry and finite element mesh for modeling the melting and dripping behavior of low molecular weight (23K) atactic polypropylene.

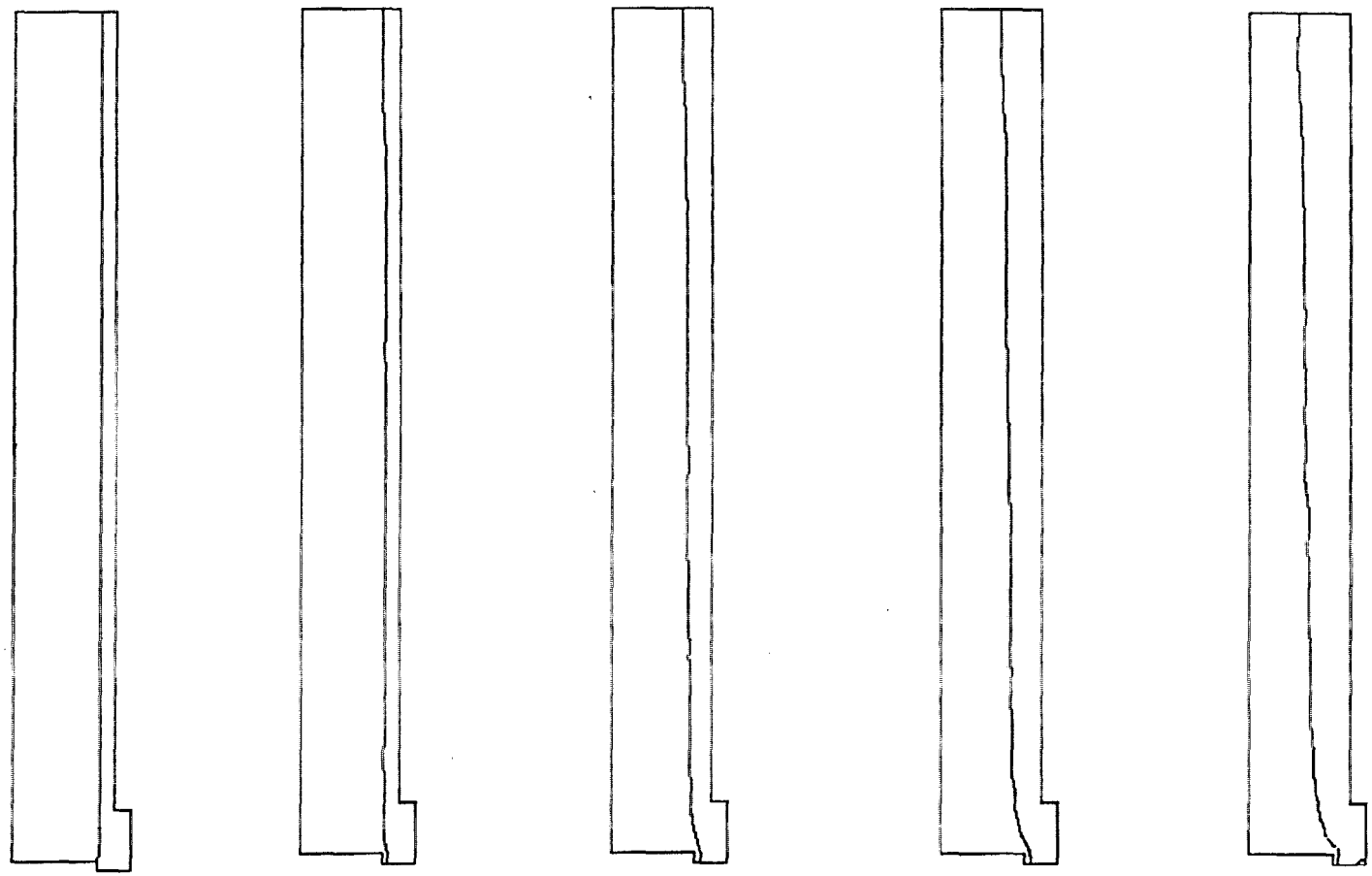

Figure 8. Calculated profiles of 23KPP sample at 100 second intervals during melt flow at incident heat flux of 12.5 kW/m^2.

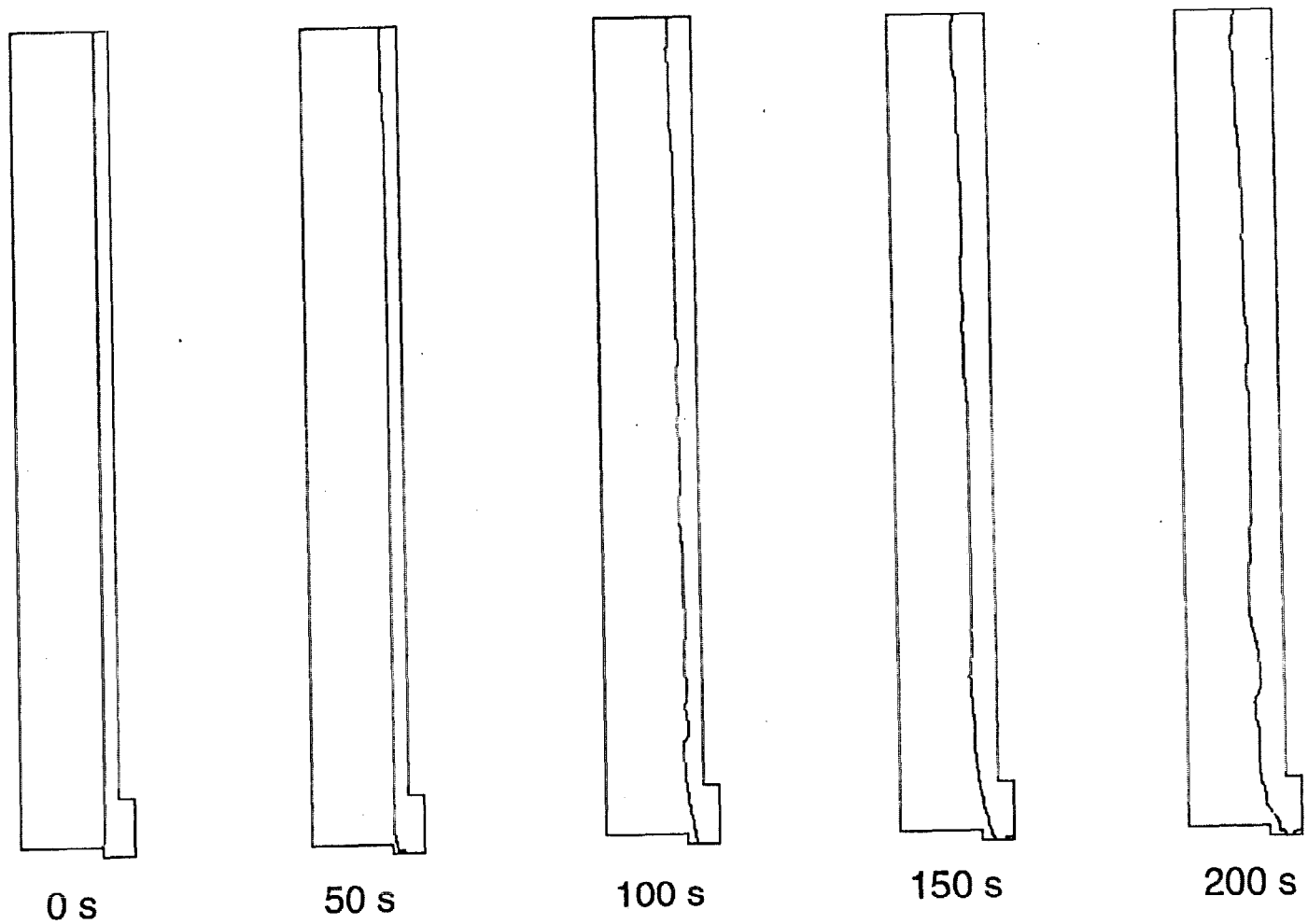

Figure 9. Calculated profiles of 23KPP sample at 50 second intervals during melt flow at an incident heat flux of 20 kW/m^2.

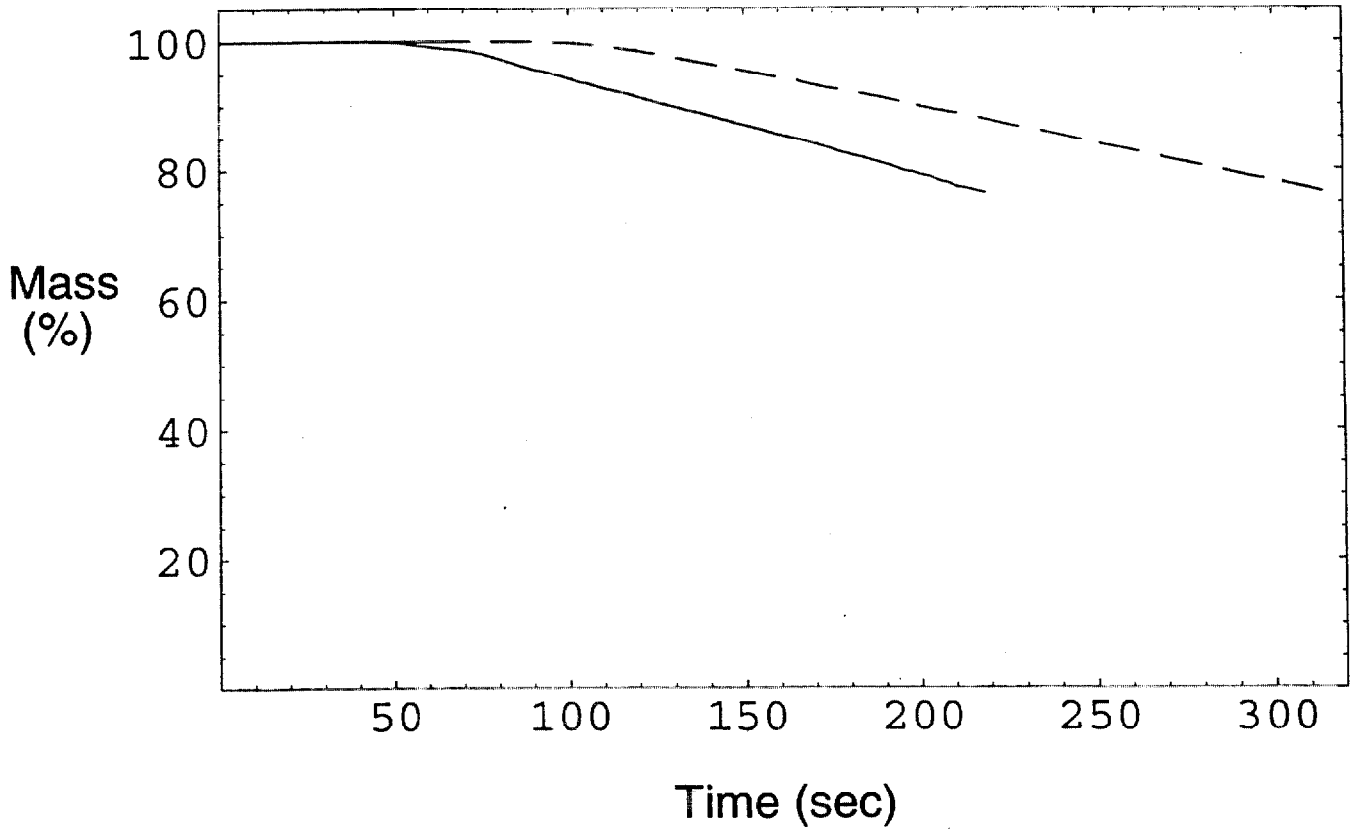

Figure 10. Percentage of initial mass remaining within the computational domain as a function of time for 23KPP exposed to 12.5 kW/m^2 (dashed line) and 20 kW/m^2 (solid line).

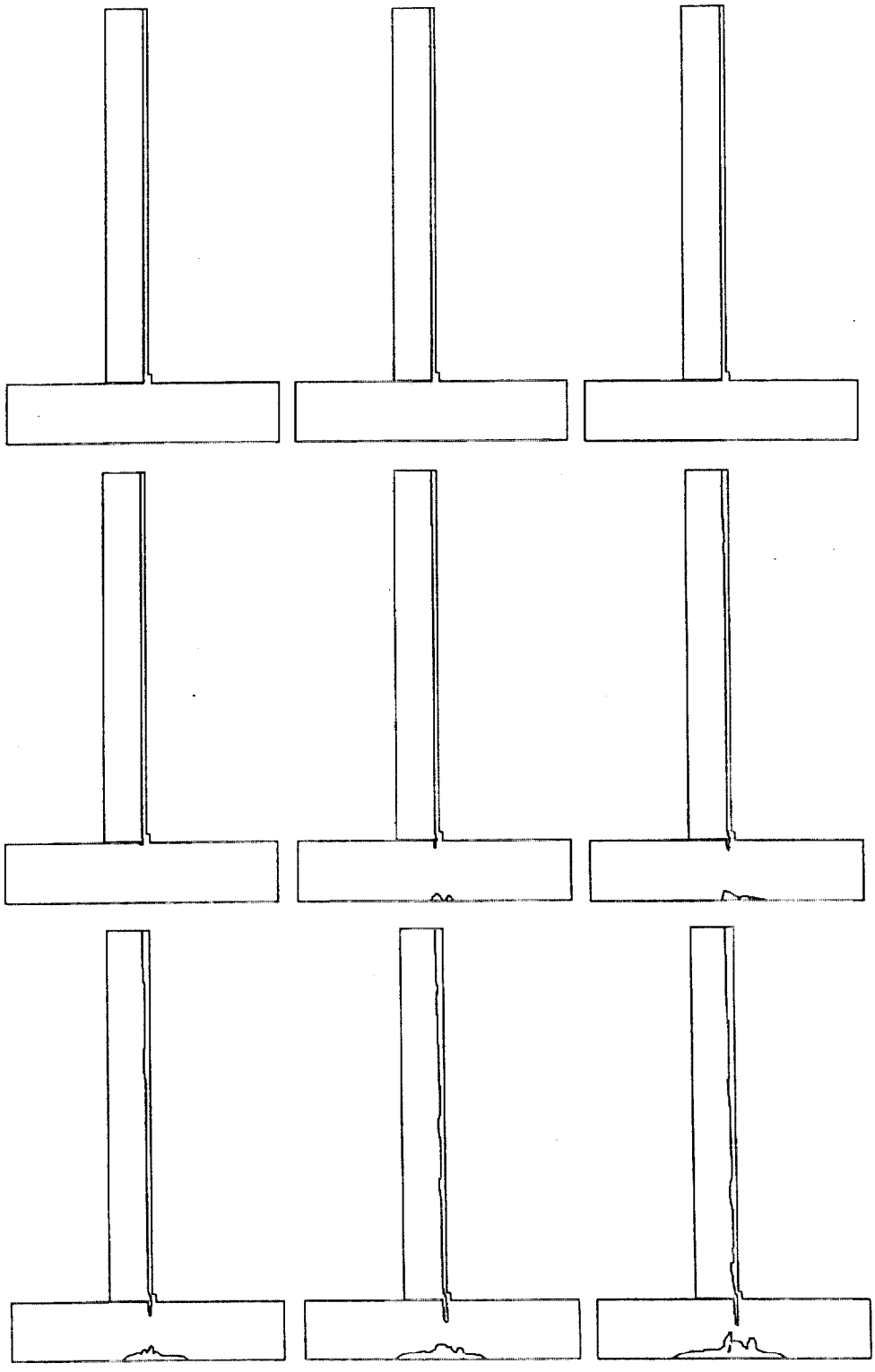

Figure 11. Profiles of 23KPP polymer boundaries including dripping into catch basin, from t=20 s to t=100 s at 10 second intervals. Incident heat on the surface of the vertical sample is 20 kW/m^2.

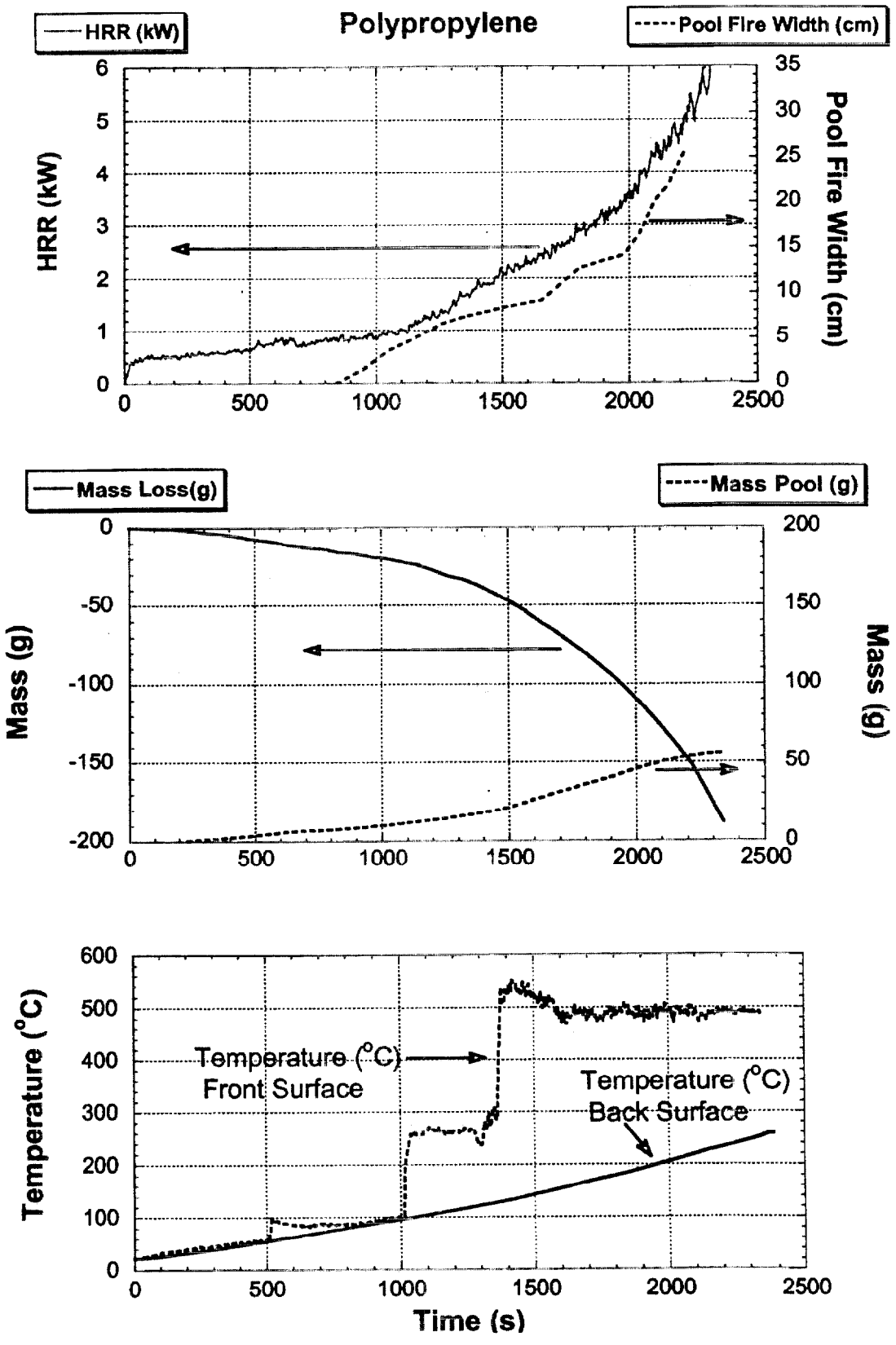

Figure 12. Melt/drip fire behavior of polypropylene; low ignition; close pool spacing.

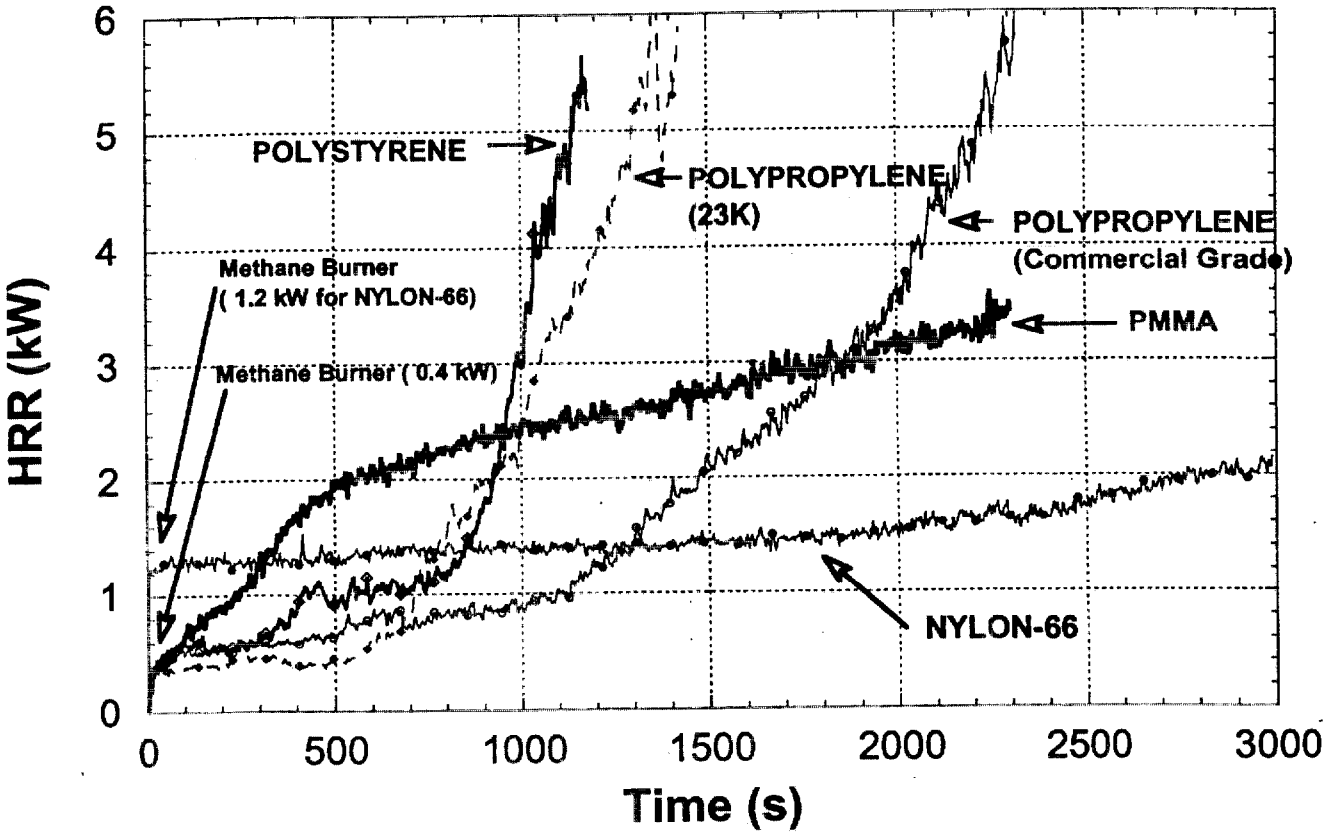

Figure 13. Heat release rate behavior of several thermoplastics, low ignition, sample close to pool.

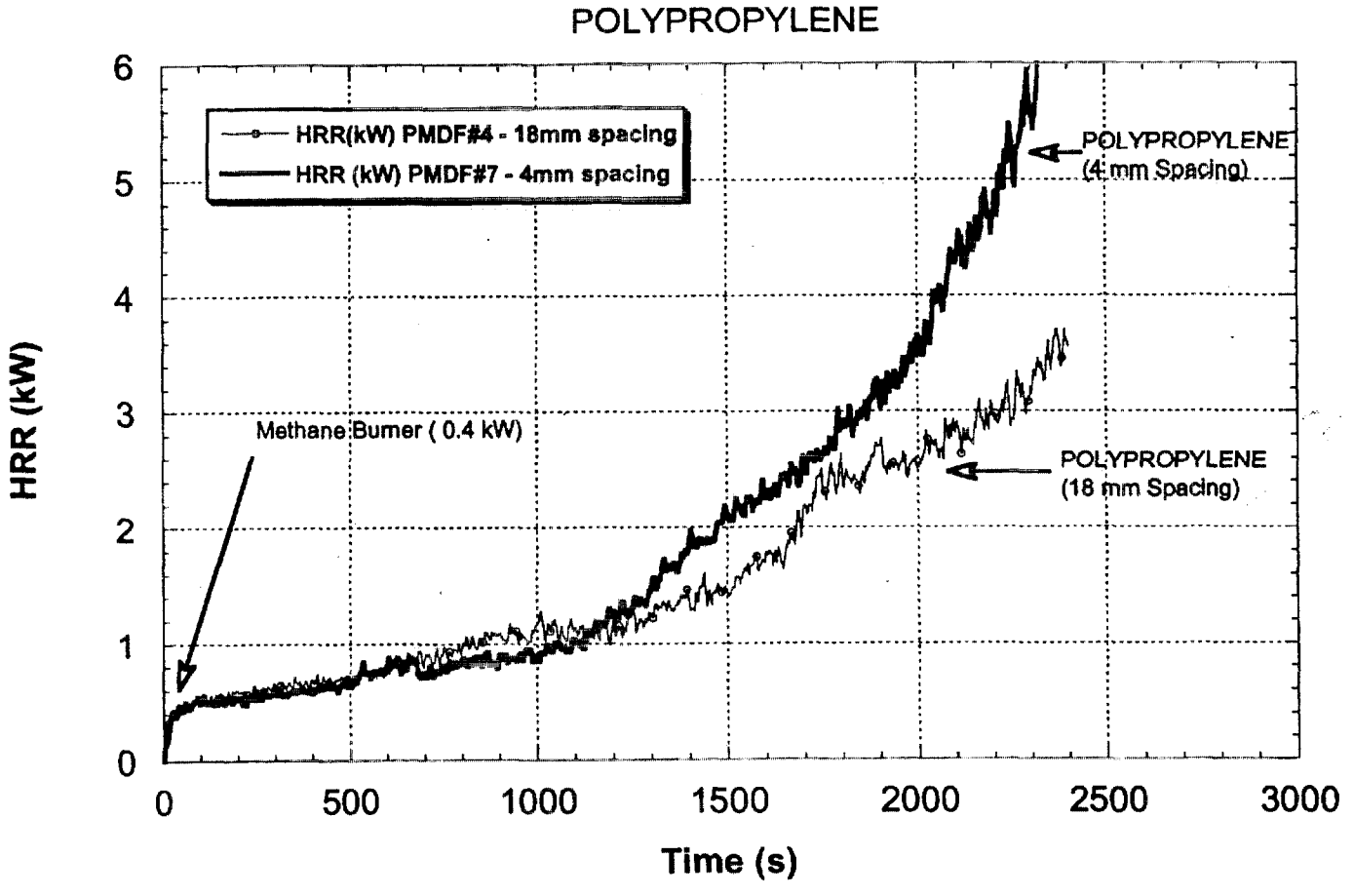

Figure 14. Effect of pool spacing on heat release rate of polypropylene

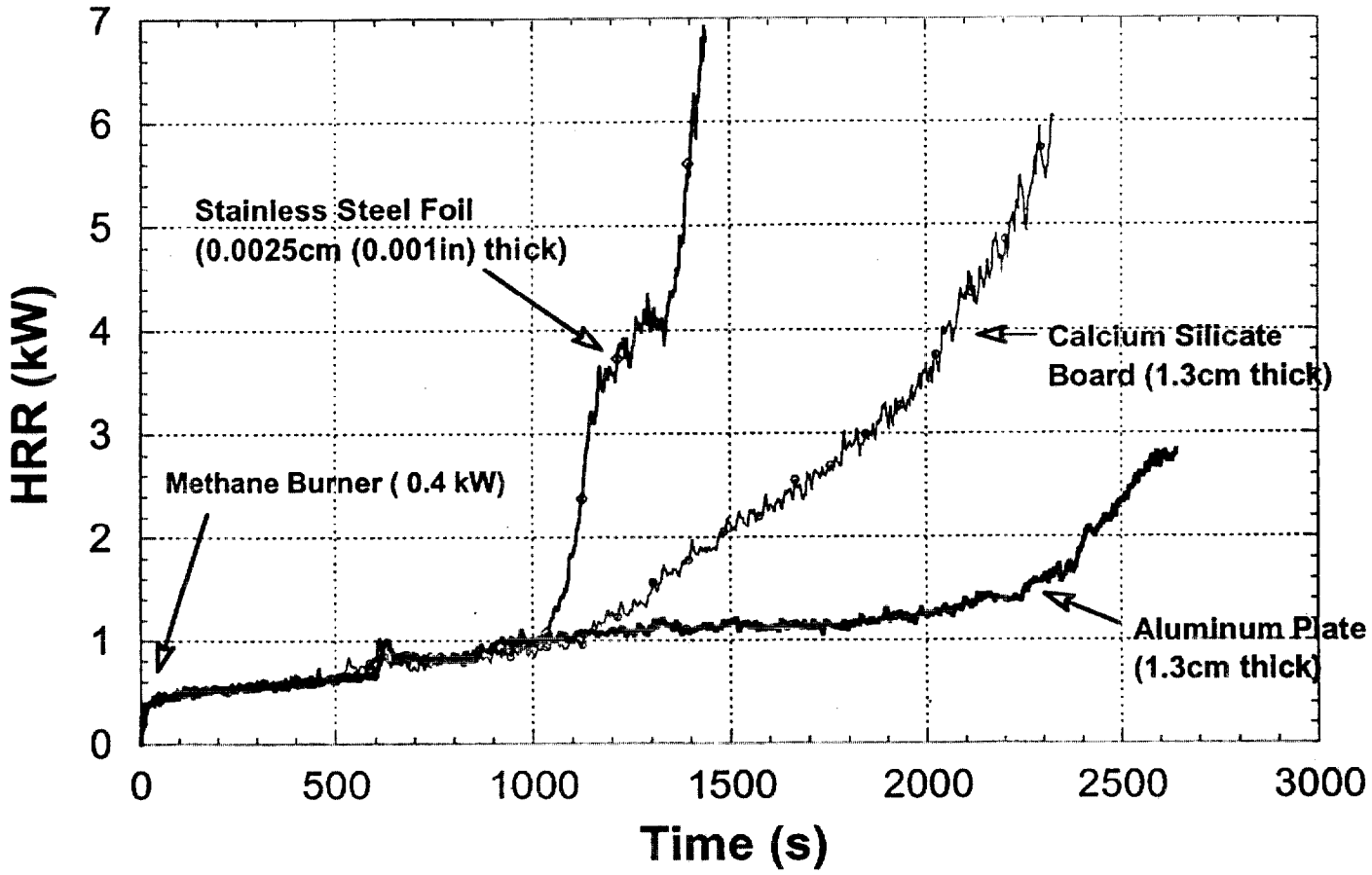

Figure 15. Effect of catch pan material on heat release rate behavior of polypropylene.